Cryptic Magmatic Skarn of the Merry Widow Deposit, Vancouver Island (NTS 092L)

R. Morris[1], **School of Earth and Ocean Sciences, University of Victoria, Victoria, British Columbia, ramorri@uvic.ca**

D. Canil, School of Earth and Ocean Sciences, University of Victoria, Victoria, British Columbia

Morris, R. and Canil, D. (2021): Cryptic magmatic skarn of the Merry Widow deposit, Vancouver Island (NTS 092L); *in* Geoscience BC Summary of Activities 2020: Minerals, Geoscience BC, Report 2021-01, p. 47–54.

Introduction

Skarn deposits are typically defined as calcsilicate assemblages that occur within or adjacent to carbonate-bearing rocks (limestone, dolostone) as a result of metamorphic and metasomatic processes, and are a major source of Fe, Au, Cu, Pb, Zn, W, Mo and Sn (Meinert et al., 2005; Ray, 2013). Skarn is generally associated with intrusions into carbonate wallrock, and the ore deposit forms from a combination of an initial thermal-metamorphic event followed by secondary metasomatic alteration from fluids of magmatic, metamorphic or meteoric origin (Meinert et al., 2005). The resulting skarn is an alteration envelope that can be mapped around the intrusion (Ettlinger and Ray, 1987). Skarn can be further classified as 1) exoskarn, which consists of the decarbonized and silicified carbonate wallrock, or 2) endoskarn, which consists of calcified and desilicified igneous rocks within the intrusion (Sangster, 1964; Meinert et al., 2005).

Less commonly discussed and not evident in outcrop is 'magmatic skarn', which occurs as a result of assimilation of Ca-rich wallrock (i.e., carbonate, calcsilicate) within the magma (Barnes et al., 2009). Earlier skarn studies on Vancouver Island, British Columbia (BC) by Sangster (1964) hinted at a potential presence of magmatic skarn, where he noted that contact metamorphism was "most striking" in metasomatized country rocks, but that "endomorphism within the pluton" was less obvious. This endomorphism was noted after observing a common occurrence of mafic margins within skarn-associated intrusions (Sangster, 1964). Such mafic margins may be a result of the initial mafic parental melt cooling along the magma chamber margin, or from fractional crystallization of mafic phases as a result of wallrock assimilation, or from a combination of these processes. If assimilation-driven fractional crystallization occurs, this would be evident by an abundance of mafic cumulates that are proximal to the wallrock contact. Studies by Barnes et al. (2009) have indicated cumulates of Ca-rich fractionates (clinopyroxene, titanite, plagioclase) within magmatic skarn. These distinct cumulates were termed 'hortite' from earlier mapping by Vogt (1916). Calcium-rich cumulates are interpreted to be a result of assimilation, where an increase in Ca within the magma from partially melted carbonate or calcsilicate wallrock induces the fractionation of calcic phases (i.e., clinopyroxene, plagioclase, titanite, apatite). If this process does occur, the latent heat produced by fractional crystallization would enhance wallrock assimilation (Taylor, 1980; De Paolo, 1981; Spera and Bohrson, 2001).

This study quantifies the extent of magmatic skarn within a well-exposed intrusion, the Coast Copper stock, that is associated with the Merry Widow Fe-skarn deposit on Vancouver Island. This paper presents the preliminary field and geochemical work completed on the magmatic skarn thus far.

Merry Widow Deposit

The Merry Widow Fe-skarn deposit occurs at the contact of Jurassic Bonanza arc intrusions with Triassic Quatsino limestone (Figure 1) in Wrangellia on northern Vancouver Island (Sangster, 1964; Lund, 1966; Ray and Webster, 1991; Nixon et al., 2011). The orebody was mined from 1957 to 1967, primarily for magnetite (MINFILE 092L 044, 045 and 046; BC Geological Survey, 2020b). Skarn mineralization at Merry Widow consists of magnetite, pyrrhotite, pyrite, arsenopyrite, cobaltite, erythrite, sphalerite and gold in a gangue of garnet, epidote, actinolite, clinopyroxene, carbonate and quartz (Ray and Webster, 1991). This mineralization is recognizable in outcrop and drillcore. However, determining the precise extent of magmatic skarn within the intrusion requires a fastidious examination of geochemical relationships in order to differentiate contaminated from pristine magmatic rock.

A number of previous studies have been completed on the geology and mineral occurrences at the Merry Widow site (Figure 2; Sangster, 1964; Lund, 1966; Ray and Webster, 1991; Nixon et al., 2011). This study focused on the petrography of dikes, plutonic rocks and carbonate wallrock, and

[1]*The lead author is a 2020 Geoscience BC Scholarship recipient.*

This publication is also available, free of charge, as colour digital files in Adobe Acrobat® PDF format from the Geoscience BC website: http://geosciencebc.com/updates/summary-of-activities/.

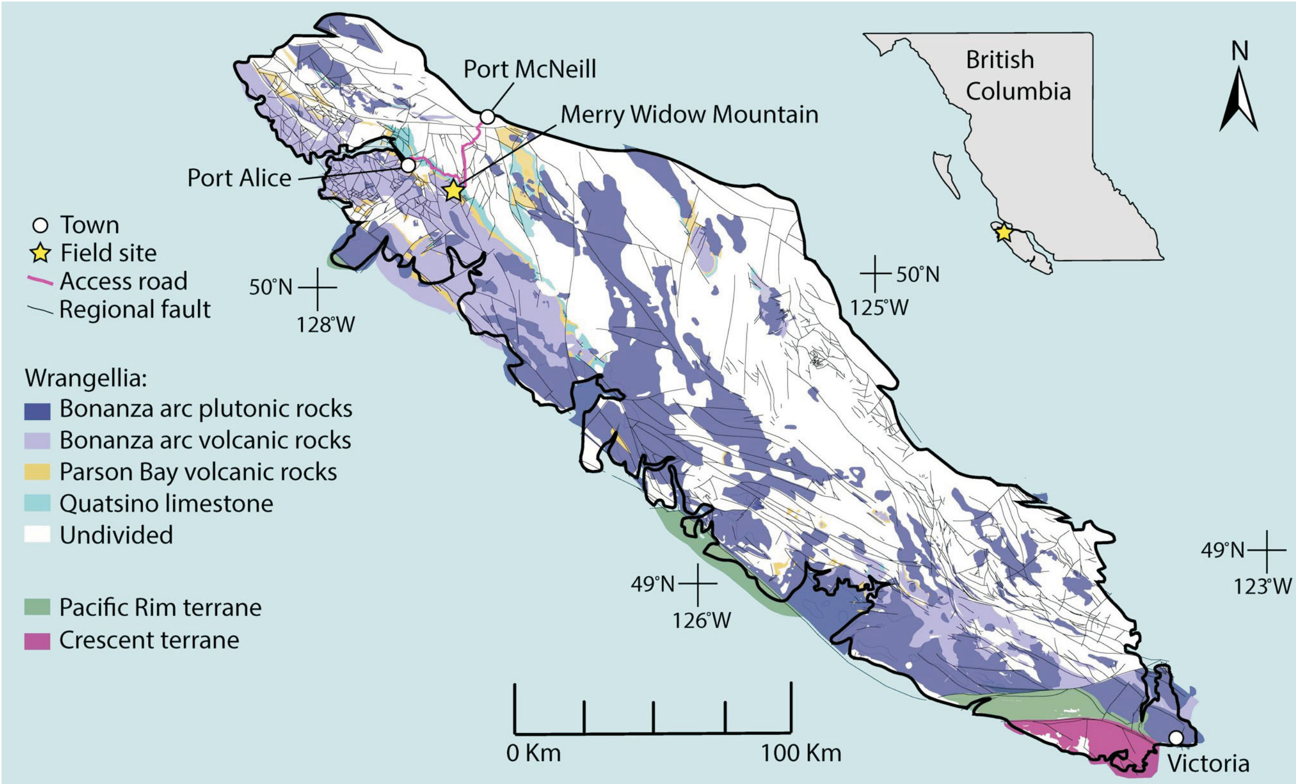

Figure 1. Regional geology of Vancouver Island from Morris and Canil (2020), showing Wrangellia and the Pacific Rim and Crescent terranes. Wrangellia is stripped of its pre- and post-Jurassic rocks, except for the Parson Bay volcanic rocks and Quatsino limestone (both Triassic), which immediately underlie the Jurassic Bonanza arc. Geological unit boundaries and faults are from the BC Geological Survey (BCGS) MapPlace dataset (BC Geological Survey, 2020a). The Merry Widow Mountain area is located within NTS 092L.

the contact relations at the site (Morris and Canil, 2020). Herein, the extent of magmatic skarn within the Coast Copper stock, the main plutonic body at the Merry Widow deposit, is quantified using samples collected during the 2019 field program that were analyzed for whole-rock geochemistry and oxygen isotopes. In addition, publicly available subsurface drillcore logs and whole-rock geochemistry data were compiled and incorporated with mapping from Morris and Canil (2020). The results reveal a far larger volume of magmatic skarn that is not evident in surface field geology.

Fieldwork

During the 2019 fieldwork, the eastern margin of the Coast Copper stock and an ~1 km transect from the pluton-wallrock contact into the interior of the pluton were mapped and sampled in detail (Figure 2; Morris and Canil, 2020). The margin of the Coast Copper stock is gabbro, with lesser amounts of monzonite. The pluton shows heterogeneities that include regions of pegmatite (plagioclase laths up to 5 cm long); spheroidal cumulates (plagioclase + clinopyroxene + magnetite + apatite + titanite) that are proximal (~200 m orthogonal) to the pluton margin; magma-mingling textures between the lesser monzonite and gabbro on a variety of scales; and thin (<0.5 m) monzonite dikes (Morris and Canil, 2020). Some regions display a greenschist-facies hydrothermal overprint, with occurrences of albitized plagioclase and chlorite.

Historical Core-Log Compilation

Publicly available core logs from 2006 and 2007 drilling programs at Merry Widow were compiled to interpret subsurface relationships between the Coast Copper stock and Quatsino limestone (Nicholson, 2006; Wesley and Nelson, 2008a). Six core logs from these drilling programs show an intersection with the plutonic margin (Figure 2), which includes two core logs from the 2006 program (MW06-08, MW06-15) and four core logs from the 2007 program (MW07-78, MW07-79, MW07-80, MW07-90; Nicholson, 2006; Wesley and Nelson, 2008a). Mapped bedding and contact exposures at the surface (Figure 2), when combined with depths of intersection of the Coast Copper stock based on drillhole trend and plunge, show the pluton margin has an orientation of ~340°/59°NE if generalized to be a planar structure. Contact relationships of the pluton at depth are shown in Figure 3, where the selected cross-section transects a vertical drillhole (MW07-78) south of the main magnetite deposit.

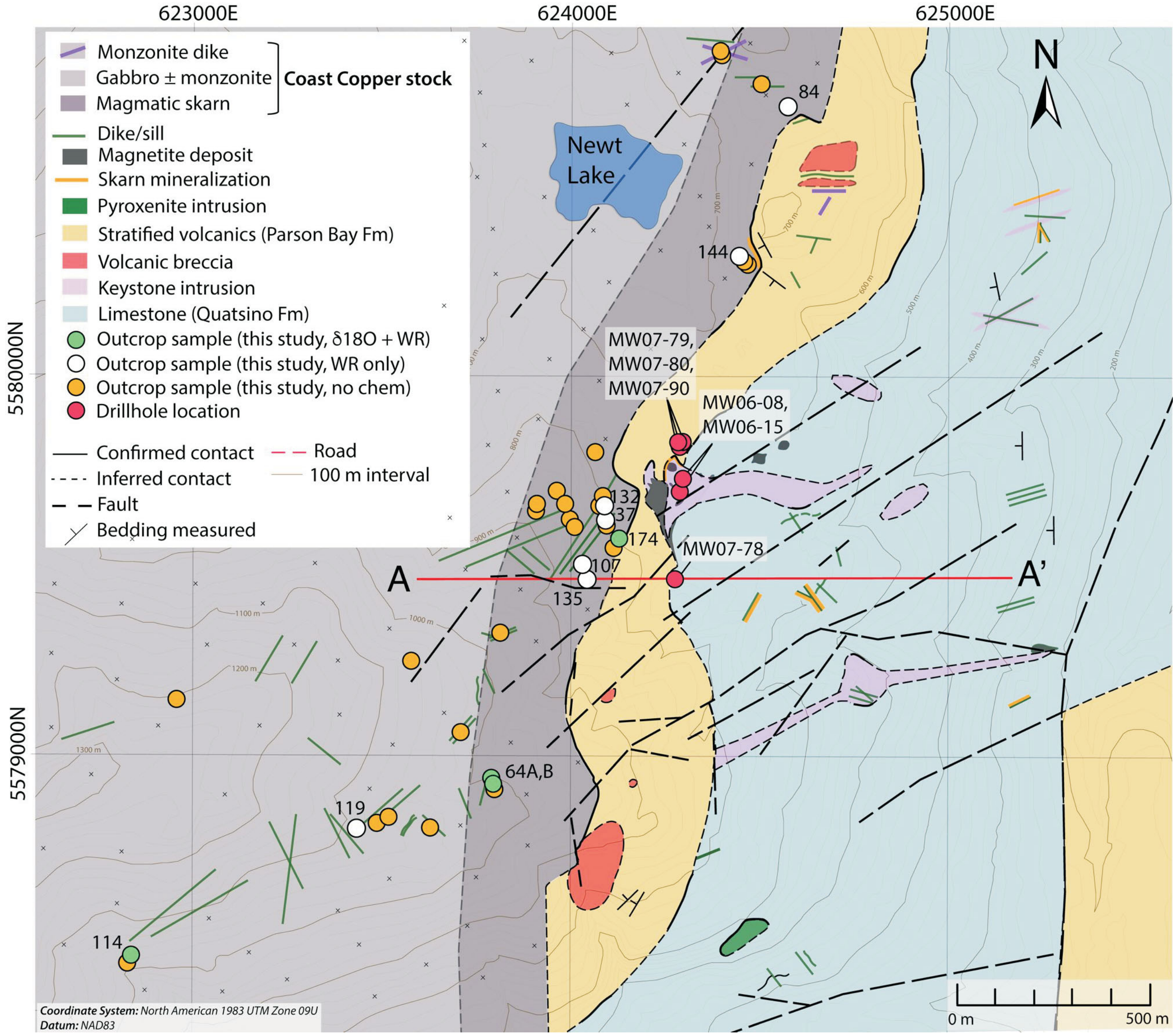

Figure 2. Detailed bedrock geology of the Merry Widow site, modified after Sangster (1964), Lund (1966), Ray and Webster (1991) and Nixon et al. (2011). Drillhole locations from Nicholson (2006) and Wesley and Nelson (2008a) are shown in red. Outcrop samples from this study are shown in white, green and orange. Gabbro collected near dikes was sampled >1 m away from dike margins and appeared fresh in outcrop and hand sample. Samples collected northeast of Newt Lake appear to have been subjected to faulting and hydrothermal alteration, and were not submitted for $\delta^{18}O$ analyses. Samples from this study were analyzed for whole-rock (WR) geochemistry (white symbol), with some samples also analyzed for $\delta^{18}O$ (green symbol). The cross-section from the A–A' transect is shown in Figure 3.

At surface, there is no exposure of the Coast Copper stock in direct contact with the Quatsino limestone (Figure 2). Core logs, however, indicate approximate true thicknesses of various units across the transition from wallrock to pluton, which includes: ~100 m of irregular exoskarn, ~10–60 m of volcanic breccia, ±3–10 m of recrystallized limestone), leading into at least ~20 m of magmatic skarn based on the authors' interpretation of core-log descriptions (Nicholson, 2006; Wesley and Nelson, 2008a). The extent of magmatic skarn from core logs is limited by sampled depths (i.e., up to a maximum of 25 m into the pluton was sampled) and is interpreted to extend beyond these sampled limits. Here, the magmatic skarn is defined based on its abundance of spheroidal mafic cumulates, which occur irregularly along the pluton margin. These cumulates consist of clinopyroxene and plagioclase, are rich in magnetite (>10%), apatite (>3%) and titanite (>1%), and produce unique geochemistry, as described below.

Magmatic Skarn Geochemistry

Whole-Rock Major- and Trace-Element Geochemistry

In this study, whole-rock major- and trace-element geochemistry are used to identify changes in the pluton due to limestone assimilation, such as increased Ca and/or de-

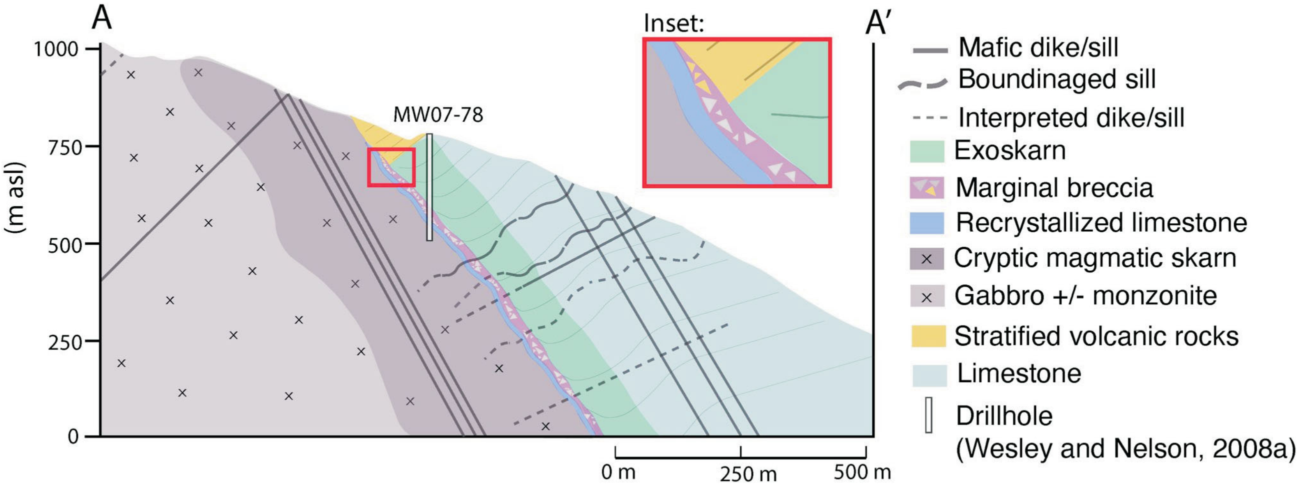

Figure 3. Cross-section A–A' (from Figure 2), representing the authors' interpretation of field relationships at depth, which are established from extrapolation of exposed bedding and contacts and from publicly available core-log data (Nicholson, 2006; Wesley and Nelson, 2008a). The extent of magmatic skarn is based on preliminary field and geochemical results.

creased Si concentrations. Three drillholes that intersected the Coast Copper stock (MW06-08, MW06-15 and MW07-79) have whole-rock major- and trace-element data determined by inductively coupled plasma–emission spectrometry (ICP-ES) that is publicly available (Nicholson, 2006; Wesley and Nelson, 2008b). Based on sample depths and the orientation of drillholes, the Coast Copper stock was intersected from its margin to the approximate orthogonal distances in each of the following drillholes: 1.2–7.5 m for MW06-08 (6 samples), 1.1–16.7 m for MW06-15 (15 samples) and 0.9–25.2 m for MW07-79 (10 samples). Core logs indicate that samples were collected at ~1 m intervals with the exception of drillhole MW07-79, in which three samples were collected <2 m from the margin and the remaining seven collected 19–25 m from the margin.

Whole-rock major-element geochemistry of the Coast Copper stock samples, collected during the 2019 field campaign (n = 11), were compiled and compared to drillcore sample results. Samples from the 2019 field campaign included 10 gabbro and 1 cumulate, which were both proximal and distal with respect to the pluton-wallrock margin (Figure 2). The orthogonal distances of outcrop samples collected from the pluton-wallrock margin were calculated for spatial comparison with chemistry of the drillcore samples, using a regionally generalized planar plutonic margin that strikes ~340°/59°NE, based on core logs (Nicholson, 2006; Wesley and Nelson, 2008a).

The magmatic skarn intersected in drillcore displays unique chemical trends of increasing P_2O_5 and TiO_2 with increasing distance from the pluton-wallrock contact. Typical mafic igneous values of P_2O_5 (<0.5 wt. %) and TiO_2 (<2 wt. %) are achieved between 200 and 500 m from the pluton-wallrock contact, as indicated in outcrop sample chemistry (Figure 4). Results also show an overall increase in FeO*, MgO and CaO with increasing distance from the pluton-wallrock contact. However, the boundary from contaminated (magmatic skarn) to pristine magmatic rock is less obvious with these elements, as high concentrations are sustained in the most distal samples. The chemical compositions observed in distal drillcore samples (~20 m inward from the margin) are either similar to, or trend toward, those of the cumulate sampled in outcrop approximately 200 m orthogonal from the pluton margin (Figure 4). Drillcore analytical reports provided no Si concentrations, so it is assumed that magmatic skarn is low in SiO_2, similar to the cumulate (<45 wt. % SiO_2).

The irregularity of major-element abundances in drillcore and in sampled outcrops along the pluton margin is interpreted to be a result of simultaneous assimilation and fractional crystallization. This is obvious in drillcore samples from MW06-08 and MW06-15, which display similar trends and were well sampled, with continuous data from 1 to 20 m, as demonstrated by the increasing TiO_2. However, samples from MW07-79 do not show this trend, likely due to no sample collection between 2 and 19 m from the margin. In addition, MW06-08 and MW06-15 were drilled at similar locations within the main pit, whereas MW07-79 was drilled north of the main pit (Figure 2).

Overall, major- and trace-element chemistry indicates substantial accumulation of magnetite (up to 30%), titanite and apatite within intervals of magmatic skarn at the margin of the Coast Copper stock, some of which are marked by increasing Co concentration (Figure 4), a metal also enriched in exoskarn at the Merry Widow deposit (Ray and Webster, 1991). No surface samples collected during the 2019 field campaign were analyzed for Co, so the extent of Co concentrations is currently limited to the publicly available geochemical data from drillcore samples (Nicholson, 2006; Wesley and Nelson, 2008b).

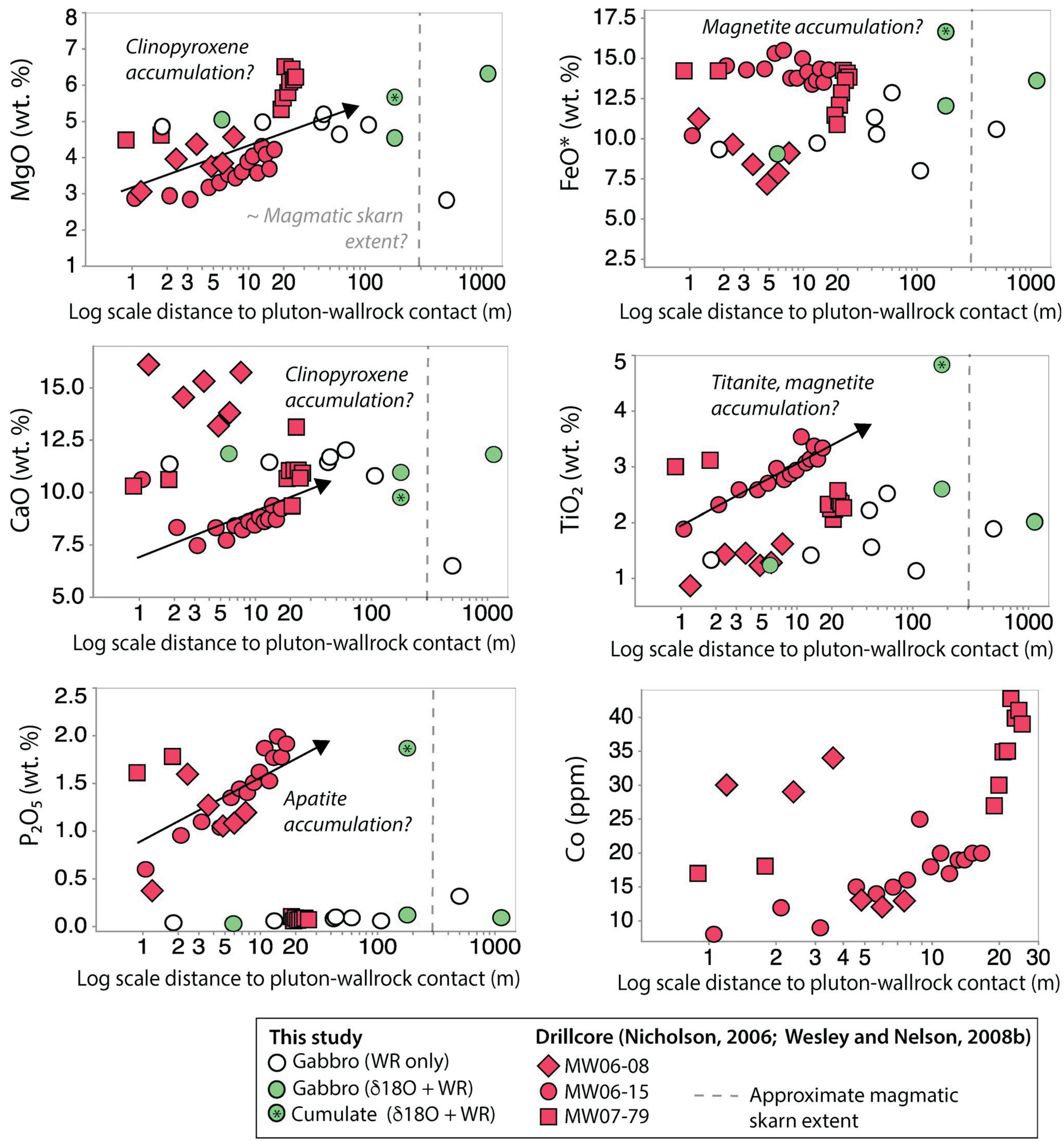

Figure 4. Major- and trace-element concentrations of whole-rock (WR) pluton samples from drillcore (published in Nicholson, 2006; Wesley and Nelson, 2008b) and this study, plotted against the approximate orthogonal distance from the pluton-wallrock margin. Trace-element chemistry is only available from drillcore data. Samples intersected by drilling are shown in red (drillcore symbols).

Due to the nature of skarn deposits, it is likely that the margin of the pluton experienced metasomatism in some regions, a factor that should be considered when evaluating whole-rock chemistry. Nevertheless, the high levels of P_2O_5 in magmatic skarn suggest accumulation of at least 5% apatite, also noted previously in petrographic examination of cumulates in the pluton (Morris and Canil, 2020). Accessory phases such as titanite and apatite are relatively resistant to metasomatic replacement and, in this instance, can be interpreted as a good indicator of carbonate assimilation.

Oxygen Isotopes

Whole-rock samples collected from the 2019 field campaign were analyzed for $\delta^{18}O$ to quantitively measure the extent of assimilation within the Coast Copper stock, which ultimately affects major-element geochemical trends (Figure 4). Four samples from the Coast Copper stock were analyzed for $\delta^{18}O$ at the University of Oregon Stable Isotope Laboratory using methods given in Watts et al. (2019). The submitted samples included a proximal gabbro <10 m from the margin (sample 174), a distal gabbro ~1 km from the margin (sample 114), a cumulate (sample 64B) and the cumulate host (sample 64A; Figure 2). In addition, two Quatsino limestone wallrock samples, unaltered and collected off site, were analyzed for $\delta^{18}O$ at the University of Victoria using isotope-ratio mass spectrometry (IRMS). Methods for limestone $\delta^{18}O$ analyses involved heating sample powders (<1.0 mg) and standards (IAEA-603, IAEA-CO-8 and one internal standard) at 90°C overnight in borosilicate reaction vials to remove volatiles. Vials were placed in a heated block and samples were dissolved with ~15 drops of 100% H_3PO_4 and allowed to react for a minimum of 1 hour. The resulting CO_2 gas was measured on a Sercon Ltd. 20-22 gas-source mass spectrometer with a Gas Box 2 front end. Results were reported relative to Vienna Standard Mean Ocean Water (VSMOW). Precision, based upon measurement of the internal standard, is 0.2 per mille (‰) for $\delta^{18}O$ (1σ; Vanwieren, 2019).

The gabbro $\delta^{18}O$ values range from 3.8 to 13.3‰ (Figure 5) and are highly variable compared to the narrow range of 5.5–5.9‰ for $\delta^{18}O$ in mantle-derived basalts (Bindeman, 2008). Values of $\delta^{18}O$ above 5.9‰ may indicate assimilation of the Quatsino limestone ($\delta^{18}O$ ~22‰; Figure 5) or low-temperature (<100°C) hydrothermal alteration, whereas values below 5.5‰ may indicate assimilation of hydrothermally altered material, high-temperature hydrothermal alteration or a high modal percentage of minerals with low $\delta^{18}O$, such as magnetite ($\delta^{18}O$ ~3.5‰; Cartwright and Barnicoat, 1999; Bindeman, 2008). Preliminary examination suggests limestone assimilation may be evident in a fresh proximal gabbro with $\delta^{18}O$ of 8.7‰ reported <10 m from the plutonic margin (sample 174; Figures 2, 5), as well as within the cumulate host gabbro, as indicated by a sample (sample 64A) taken ~200 m from the margin that has a highly enriched $\delta^{18}O$ value of 13.3‰. Low $\delta^{18}O$ signatures in both the sampled cumulate (sample 64B) and distal gabbro (sample 114) may be a result of the high abundance of magnetite (~30%) within these samples. Future additional $\delta^{18}O$ analyses from fresh outcrop will provide a better representation and coverage of gabbro $\delta^{18}O$ within the Coast Copper stock to help in understanding the extent of magmatic skarn and the process behind its generation.

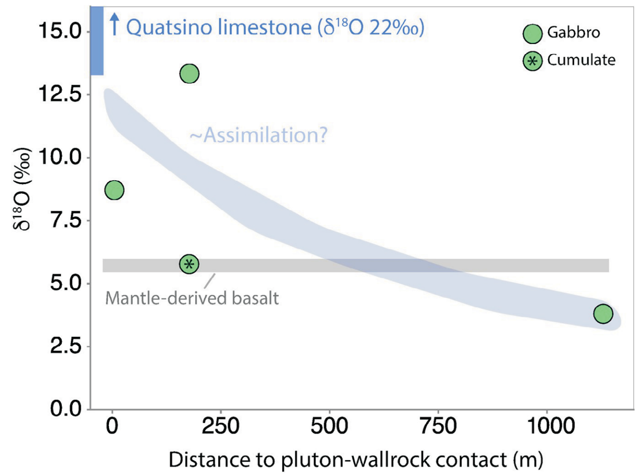

Figure 5. Oxygen-isotope results from Coast Copper stock gabbro plotted against the distance orthogonal to the pluton-wallrock contact with Quatsino limestone. Results show a variable range in comparison to typical mantle-derived basalts (Bindeman, 2008). Results suggest possible assimilation with $\delta^{18}O$-enriched wallrock, such as the Quatsino limestone. Enriched $\delta^{18}O$ can also occur from low-temperature hydrothermal alteration. Depleted $\delta^{18}O$ may indicate high modal percentages of minerals with low $\delta^{18}O$ (i.e., ~3.5‰ in magnetite) or high-temperature hydrothermal alteration. Oxygen isotope values are standardized to Vienna Standard Mean Ocean Water (VSMOW).

Conclusions

This paper summarizes preliminary results to quantify the size and extent of magmatic skarn within the Coast Copper stock at the Merry Widow deposit from surface geology (Morris and Canil, 2020) and core logs, and to examine its formation using $\delta^{18}O$ and whole-rock geochemistry. The transition from wallrock to pluton at Merry Widow is characterized by ~100 m of irregular exoskarn, ~10–60 m of volcanic breccia, ±3–10 m of recrystallized limestone and potentially >200 m of magmatic skarn. Assimilation of Triassic Quatsino limestone by the ~197 Ma Coast Copper stock enriches the gabbro $\delta^{18}O$ and results in a pluton margin characterized by an accumulation of magnetite, apatite and titanite. More $\delta^{18}O$ analyses will be completed for a better representation and coverage of the magmatic skarn within the Coast Copper stock. Results from this research can be used to estimate the extent of magmatic skarn and possible mineralization within other Fe-skarn deposits located throughout Wrangellia.

Acknowledgments

This project was supported by Geoscience BC scholarships (RM) and a Natural Sciences and Engineering Research Council of Canada (NSERC) Discovery Grant (DC). The authors thank G. Simandl for his comments and suggestions. They also thank J. Husson for access to his IRMS facility and J. Lei for analytical assistance.

References

Barnes, C.G., Prestvik, T., Yujia, L., McCulloch, L., Yoshinobu, A.S. and Frost, C.D. (2009): Growth and zoning of the Hortavær intrusive complex, a layered alkaline pluton in the Norwegian Caledonides; Geosphere, v. 5, p. 286–301, URL <http://doi.org/10.1130/GES00210.1>.

BC Geological Survey (2020a): MapPlace GIS internet mapping system; BC Ministry of Energy, Mines and Low Carbon Innovation, BC Geological Survey, MapPlace website, URL <http://www.MapPlace.ca> [October 2020].

BC Geological Survey (2020b): MINFILE BC mineral deposits database; BC Ministry of Energy, Mines and Low Carbon Innovation, BC Geological Survey, URL <http://minfile.ca/> [October 2020].

Bindeman, I. (2008): Oxygen isotopes in mantle and crustal magmas as revealed by single crystal analysis; Mineralogical Society of America Reviews in Mineralogy, v. 30, p. 157–186, URL <http://doi.org/10.2138/rmg.2008.69.12>.

Cartwright, I. and Barnicoat, A.C. (1999): Stable isotope geochemistry of alpine ophiolites: a window to ocean-floor hydrothermal alteration and constraints on fluid-rock interaction during high-pressure metamorphism; International Journal of Earth Sciences, v. 88, p. 219–235, URL <https://doi.org/10.1007/s005310050261>.

De Paolo, D.J. (1981): Trace element and isotopic effects of combined wallrock assimilation and fractional crystallization; Earth and Planetary Science Letters, v. 53, p. 189–202, URL <https://doi.org/10.1016/0012-821X(81)90153-9>.

Ettlinger, A.D., and Ray, G.E. (1987): Gold-enriched skarn deposits of British Columbia; *in* Geological Fieldwork 1987, BC Ministry of Energy, Mines, and Petroleum Resources, Paper 1988-1, p. 263–279, URL <http://cmscontent.nrs.gov.bc.ca/geoscience/PublicationCatalogue/Paper/BCGS_P1988-01.pdf> [October 2020].

Lund, J.C. (1966): Structural geology of Empire mine, Empire Development Limited, Port McNeil, British Columbia; M.Sc. thesis, The University of British Columbia, URL <http://hdl.handle.net/2429/37080> [October 2020].

Meinert, L.D., Dipple, G.M., and Nicolescu, S. (2005): World skarn deposits; Society of Economic Geologists, Economic Geology 100th Anniversary Volume, p. 299–336, URL <https://doi.org/10.5382/AV100.11>.

Morris, R. and Canil, D. (2020): Skarn mineralization along magma-carbonate contacts in the Merry Widow Mountain area, Vancouver Island, British Columbia (NTS 092L); *in* Geoscience BC Summary of Activities 2019: Minerals, Geoscience BC, Report 2020-01, p. 5–12, URL <http://www.geosciencebc.com/i/pdf/SummaryofActivities2019/Minerals/Sch_Morris_Minerals_SOA2019.pdf> [October 2020].

Nicholson, G. (2006): Assessment report on the diamond drilling on the Merry Widow property, Nanaimo Mining Division, Vancouver Island; BC Ministry of Energy, Mines and Low Carbon Innovation, Assessment Report 28863, 423 p., URL <https://aris.empr.gov.bc.ca/ArisReports/28863.PDF> [October 2020].

Nixon, G.T., Snyder, L.D., Payie, G.J., Long, S., Finnie, A., Orr, A.J., Friedman, R.M., Archibald, D.A., Orchard, M.J., Tozer, E.T., Poulton, T.P. and Haggart, J.W. (2011): Geology, geochronology, lithogeochemistry and metamorphism of the Alice Lake area, northern Vancouver Island, NTS 092L/06 and part of 092L/03; BC Ministry of Energy, Mines and Low Carbon Innovation, BC Geological Survey, Geoscience Map 2011-4, scale 1:50 000, URL <http://cmscontent.nrs.gov.bc.ca/geoscience/PublicationCatalogue/GeoscienceMap/BCGS_GM2011-04.pdf> [October 2020].

Ray, G.R. (2013): A review of skarns in the Canadian Cordillera; BC Ministry of Energy, Mines and Low Carbon Innovation, BC Geological Survey, Paper 2013-08, 52 p., URL http://cmscontent.nrs.gov.bc.ca/geoscience/PublicationCatalogue/OpenFile/BCGS_OF2013-08.pdf [October 2020].

Ray, G.E. and Webster, I.C.L. (1991): Geology and mineral occurrences of the Merry Widow skarn camp, northern Vancouver Island; BC Ministry of Energy, Mines and Low Carbon Innovation, BC Geological Survey, Open File 1991-08, 1 map at 1:5000 scale, URL <http://cmscontent.nrs.gov.bc.ca/geoscience/PublicationCatalogue/OpenFile/BCGS_OF-1991-08.pdf> [October 2020].

Sangster, D.F. (1964): The contact metasomatic magnetite deposits of southwestern British Columbia, Ph.D. thesis, The University of British Columbia, URL <https://open.library.ubc.ca/cIRcle/collections/ubctheses/831/items/1.0053070> [October 2020].

Spera, F.J., and Bohrson, W.A. (2001): Energy-constrained open-system magmatic processes I: general model and energy-constrained assimilation and fractional crystallization (EC-AFC) formulation; Journal of Petrology, v. 42, p. 999–1018, URL <https://doi.org/10.1093/petrology/42.5.999>.

Taylor, H.P. (1980): The effects of assimilation of country rocks by magmas on $^{18}O/^{16}O$ and $^{87}Sr/^{86}Sr$ in igneous rocks; Earth and Planetary Science Letters, v. 47, p. 243–254, URL <https://doi.org/10.1016/0012-821X(80)90040-0>.

Vanwieren, C.S. (2019): Characterizing the Triassic/Jurassic boundary through stratigraphy of northern Vancouver Island carbonates; B.Sc. thesis, University of Victoria.

Vogt, T. (1916): Petrographisch-chemische studien an einigen assimilations-gesteinen der Nordnorwegishen gebirgskette; Videnskapsselskapets Skrifter, v. 1, p. 1–33.

Watts K.E., John, D.A., Colgan, J.P., Henry, C.D., Bindeman, I.N. and Valley, J.W. (2019): Oxygen investigation of silicic magmatism in the Stillwater caldera complex, Nevada: generation of large-volume, low $\delta^{18}O$ rhyolite tuffs and assessment of their regional context in the Great Basin of the western United States; GSA Bulletin, v. 131, p. 1133–1156, URL <https://doi.org/10.1130/B35021.1>.

Wesley, R. and Nelson, M. (2008a): Diamond drilling, geochemical and geophysical assessment report for the 2007 program at the Merry Widow project, Nanaimo Mining Division, Vancouver Island; BC Ministry of Energy, Mines and Low Carbon Innovation, Assessment Report 30002a, 242 p., URL <https://aris.empr.gov.bc.ca/ArisReports/30002A.PDF> [October 2020].

Wesley, R. and Nelson, M. (2008b): Diamond drilling, geochemical and geophysical assessment report for the 2007 program at the Merry Widow project, Appendix 3 – Analytical certificates, Nanaimo Mining Division, Vancouver Island; BC Ministry of Energy, Mines and Low Carbon Innovation, Assessment Report 30002b, 589 p., URL <https://aris.empr.gov.bc.ca/ArisReports/30002B.PDF> [October 2020].